Biophysical Journal Volume 107 October 2014 1970–1979

Article

The Role of Solution Conditions in the Bacteriophage PP7 Capsid Charge Regulation

Rikkert J. Nap,[1] Anže Lošdorfer Božič,[2] Igal Szleifer,[1,*] and Rudolf Podgornik[3,4,5,*]

[1]Department of Biomedical Engineering, Department of Chemistry, and Chemistry of Life Processes Institute, Northwestern University, Evanston, Illinois; [2]Max Planck Institute for Biology of Ageing, Cologne, Germany; [3]Department of Theoretical Physics, Jožef Stefan Institute, Ljubljana, Slovenia; [4]Department of Physics, Faculty of Mathematics and Physics, University of Ljubljana, Ljubljana, Slovenia; and [5]Department of Physics, University of Massachusetts, Amherst, Massachusetts

ABSTRACT We investigate and quantify the effects of pH and salt concentration on the charge regulation of the bacteriophage PP7 capsid. These effects are found to be extremely important and substantial, introducing qualitative changes in the charge state of the capsid such as a transition from net-positive to net-negative charge depending on the solution pH. The overall charge of the virus capsid arises as a consequence of a complicated balance with the chemical dissociation equilibrium of the amino acids and the electrostatic interaction between them, and the translational entropy of the mobile solution ions, i.e., counterion release. We show that to properly describe and predict the charging equilibrium of viral capsids in general, one needs to include molecular details as exemplified by the acid-base equilibrium of the detailed distribution of amino acids in the proteinaceous capsid shell.

INTRODUCTION

Electrostatic interactions in their many guises play a fundamental role across different nanosystems (1,2). Viruses are one prominent example of a system where long-range interactions between charges appear in different parts of their lifecycle, influencing for instance the capsid stability and assembly, as well as genome packaging and ejection (3). Although the role of surface charges on the capsid/proteins have been taken into account to various degrees (Šiber et al. (3) and references therein), there have been few attempts to capture the effects of acid-base equilibrium on the sign and magnitude of the effective capsid charges as a function of solution parameters such as pH and salt ionic strength. Noteworthy in this regard are the works by Prinsen et al. (4) and Kegel and van der Schoot (5), who studied the structure and self-assembly of virus coat proteins as a function of pH and ionic strength.

Viruses and viruslike particles often carry large surface charges, making surface charge density an important system parameter (6). In experiments, however, one usually does not directly modify the charge on a capsid or a nanoparticle itself, but instead varies the pH of the solution, which in turn influences and regulates the charge of the proteinaceous shell of the virus (7–9).

Environmental conditions (such as ionic strength, pH, temperature, …) are known to affect the stability of nanoparticles and viruses (10), and the solution pH in particular was found to influence several of its aspects. For instance, very recent experimental data (11) show that the electrophoretic mobility and thus the total charge of cowpea chlorotic mottle viruses changes from positive to negative values as a function of pH and ionic strength, profoundly affecting the stability of the capsid. In addition, study of the mechanical stability of a norovirus capsid (12) concluded that its compliance increases with basic pH, along with an increase in the capsid diameter; the changes were attributed to an underlying weakening of the capsomer-capsomer interaction and to related conformational changes of the capsomers. Several studies also examined the assembly and disassembly of different viruses as a function of the solution pH and ionic strength (8,9,13), and found that single-walled shells appear only in a certain range of pH values. The efficiency of encapsidation in nanoparticle-templated assembly of viruslike nanoparticles (14) is also a strong function of the surface charge density (15,16).

Because the effects of changing pH and varying the ionic strength of the solution on the capsid charge remain largely unexplored, it is our goal in this study to elucidate the details of this dependence, with which we hope to gain some insight into the pH and ionic strength range of stability for viral capsids and viruslike nanoparticles.

MODEL

We studied the effects of pH on surface charge density of the capsid of the RNA bacteriophage PP7 (RCSB Protein Data Bank (PDB) entry PDB:1DWN). We chose this phage because its capsid carries no charged protein tails on the interior surface of the capsid. Indeed the protein N-tails can have significant charge that is important for viral genome

Submitted March 25, 2014, and accepted for publication August 26, 2014.

*Correspondence: igalsz@northwestern.edu or podgornik@physics.umass.edu

Editor: Alan Grodzinsky.

0006-3495/14/10/1970/10 $2.00

http://dx.doi.org/10.1016/j.bpj.2014.08.032

encapsidation, but are in general disordered and only partially observed in structure determination of empty capsids (17).

The capsid (Fig. 1) is modeled as a sphere of a fixed thickness and the interior and exterior radii of the capsid are determined from the capsid mass distribution as described in Lošdorfer Božič et al. (6). The capsid of the phage has an inner radius of $R_{\text{in}} = 11.8$ nm and an outer radius of $R_{\text{out}} = 13.8$ nm; the capsid thickness is consequently $\delta = 2$ nm.

For capsid proteins we only consider those amino acids that are exposed on the outer (epitopal) and inner (hypotopal) surfaces of the capsid, i.e., amino acids that are in contact with the solution, which are by assumption the only ones that contribute to the outer and inner surface charge densities of the virus capsid. Our choice of interior/exterior amino acids is by no means unique, and the definitions used could vary. Nevertheless, this model can be consistently applied to different capsids, and the effects of varying the number of epi- and hypotopal amino acids contributing to the inner and outer surface charges can be estimated quantitatively. In what follows, we also assume that dissociable amino acids are uniformly distributed on the outer and inner surfaces.

The charge of the virus capsid originates from the deprotonated carboxylate

$$RCOOH \rightleftharpoons RCOO^- + H^+$$

on the side chains of aspartic and glutamic acid, the deprotonated hydroxyl of the phenyl group of tyrosine

$$ROH \rightleftharpoons RO^- + H^+,$$

and from the protonated amine group of arginine and lysine,

$$RNH_2^+ \rightleftharpoons RNH + H^+ \text{ and } RNH_3^+ \rightleftharpoons RNH_2 + H^+.$$

The protonated state of the secondary amine of histidine could also contribute to the charge of the capsid. Inasmuch as histidine is not present in the bacteriophage of PP7, we did not take it into account. Cysteine has a thiol functional end group that is a weak acid (see Table S2 in the Supporting Material), but this amino acid is usually not considered to be an acid because the thiol group is often reactive and can form disulfide bonds. Therefore, we separately consider two cases:

1. With the protonation of the amino-acid cysteine taken into account, and
2. With the cysteine protonation not taken into account.

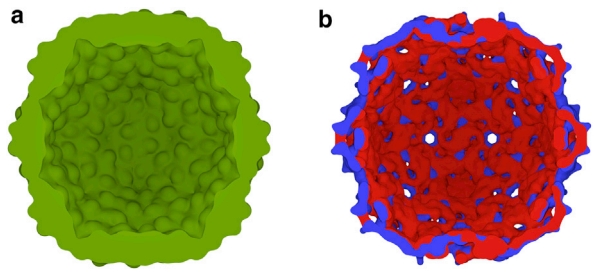

FIGURE 1 The capsid of PP7 from VIPERdb (http://viperdb.scripps.edu/). (*a*) Cross section of the capsid mass distribution constructed from PDB:1DWN. The drawing was constructed with a procedure described in detail in Šiber et al. (3). (*b*) Cross section of capsid charge distribution of the same virus. The three-dimensional representation is again constructed as described in Šiber et al. (3). The three-dimensional representation separately represents negative (*blue*) and positive (*red*) charge densities. To clearly show them both (inasmuch as the negative and positive charge distributions overlap), the positive and negative distributions are infinitesimally shifted with respect to each other, so that on the right (*left*) half of the three-dimensional representation, the positive (negative) distribution is infinitesimally closer to the viewer. To see this figure in color, go online.

The Helmholtz free energy for this system is composed of the contribution stemming from the chemical equilibrium of the dissociable surface amino-acid groups, the contribution of the entropy of the mobile ionic species, and the contribution from electrostatic interaction energy. It can be written as (18,19)

$$\begin{aligned}\beta F = \sum_{i=\{\text{in,out}\}} A_i \Bigg[& \sum_k \sigma_k^i \Big(f_k^i \ln f_k^i + (1-f_k^i)\ln(1-f_k^i) \\ & + \beta f_k^i \mu^{\ominus}_{A^-,k} + \beta(1-f_k^i)\mu^{\ominus}_{AH,k} \Big) + \sum_l \sigma_l^i \Big(g_l^i \ln g_l^i \\ & + (1-g_l^i)\ln(1-g_l^i) + \beta g_l^i \mu^{\ominus}_{BH^+,l} + \beta(1-g_l^i)\mu^{\ominus}_{B,l} \Big) \\ & + \sum_\alpha \int \mathrm{d}r G^i(r) \rho_\alpha^i(r) \left(\ln \rho_\alpha^i(r) v_w - 1 + \beta \mu_\alpha^{\ominus} \right) \\ & + \beta \int \mathrm{d}r G^i(r) \left(\rho_q^i(r)\psi^i(r) - \frac{1}{2}\varepsilon_r \varepsilon_0 \left(\nabla_r \psi^i(r)\right)^2 \right) \\ & + \beta \sigma_i \psi(R_i) \Bigg] + \beta \int \mathrm{d}r A(r) \Big(\rho_q^m(r)\psi^m(r) \\ & - \frac{1}{2}\varepsilon_m \varepsilon_0 (\nabla_r \psi^m(r))^2 \Big),\end{aligned} \tag{1}$$

where $\beta = 1/k_B T$ is the inverse temperature, and A_{in} and A_{out} are the inner and the outer surface areas of the virus capsid, respectively. The $f^i{}_k$ value corresponds to the degree of deprotonation of the carboxylic acid groups of either the aspartic acid, glutamic acid, the deprotonated state of tyrosine, or the deprotonated state of cysteine, and $g^i{}_k$ is the degree of protonation of the side-chain amine functional groups of arginine or lysine. The index i denotes either the outer (epitopal) or the inner (hypotopal) surface of the virus capsid, and the index k refers to aspartic acid, glutamic acid, tyrosine, and cysteine, and l labels arginine, or lysine. The total charge density on either the hypotopal or the epitopal surface of the capsid is given as the difference between the amount of deprotonated negatively charged acids and protonated positively charged amines,

$$\sigma_i = -e \sum_{k=\{\text{Asp,Glu,Tyr,Cys}\}} f_k^i \sigma_k^i + e \sum_{l=\{\text{Arg,Lys}\}} g_l^i \sigma_l^i, \tag{2}$$

where e corresponds to the unit of charge. Here we have assumed that the dissociable surface amino-acid groups are uniformly distributed on the outer and inner surface of the capsid and have a surface density $\sigma^i{}_k$. The first two terms in Eq. 1 describe the entropy of the deprotonated charged state and protonated neutral state of the acids, and the third and fourth terms correspond to the standard chemical potential associated with the deprotonated and protonated state of the acids, respectively. The next four terms describe the chemical free energy contribution of the chemical equilibrium associated with the protonation of the amine groups. The term involving the sum over α in the free energy expression represents the translational (mixing) entropy of the water and the mobile ionic species that include coions, counterions, protons, and hydroxide ions. The $\rho^i{}_\alpha(r)$ is the number density of molecular species α located either in the interior or exterior of the virus capsid. Here, v_w is the volume of one water molecule, and r is the radial coordinate perpendicular to the surface of the capsid. Inhomogeneities are only explicitly considered in the radial direction, r, inasmuch as the system is assumed to be homogeneous in the angular directions. The function $drG^i(r) = drA(r)/A_i$ is the volume element in the spherical coordinates divided by the area of the inner or outer surface of the capsid. This geometrical factor describes the relative change in volume depending on the distance from the capsid surface, and equals $dr(r/R_i)^2$ for a capsid. Function $A(r)$ is the area of a sphere of radius r.

The last three terms of the free energy expression account for the electrostatic contribution to the free energy (20). Here $\psi^i(r)$ is the electrostatic potential in the inner, the outer, or the shell region of the capsid. The label m refers to the shell of the capsid. The $\rho^i{}_q(r)$ value is the total charge density, composed of the density of Na^+ cations, Cl^- anions, protons H^+, and hydroxyl ions OH^-. The interior region of the virus capsid has a relative dielectric constant of 78.54 (water), being the same as in the exterior region. The virus capsid is assumed to be empty and does not contain any genetic material. The shell of the bacteriophage capsid is assumed to have a dielectric constant of 4. Other assumptions/choices made are that, in the shell, there are no free charges; and that the chemical potentials of the co- and counterions are the same for both the interior and the exterior of the bacteriophage. Namely, we assume that there is free exchange of ions between the interior and the exterior of the capsid, and therefore the two solutions are in thermodynamic equilibrium. We consider only monovalent ions. Effects due to counterion binding of divalent ions such as Mg^{2+} and Ca^{2+}, or indeed higher valency ions (21), on the charge state have not been considered.

Intermolecular excluded volume interactions are accounted for by assuming that the system is incompressible at every position

$$\phi^i_w(r) + \phi^i_{H^+}(r) + \phi^i_{OH^-}(r) + \phi^i_{Na^+}(r) + \phi^i_{Cl^-}(r) = 1. \quad (3)$$

These packing constraints are enforced through the introduction of the Lagrange multipliers $\pi^i(r)$ for both the interior and exterior of the virus capsid. Here, $\phi^i{}_\alpha(r)$ corresponds to the volume fraction of species α, which is located either in the interior of virus capsid or outside of the capsid. The volume fraction is given by $\phi^i{}_\alpha(r) = \rho^i{}_\alpha(r)v_\alpha$, with v_α corresponding to the volume of species α.

The free energy is minimized with respect to the $\rho^i{}_\alpha(r), f^i{}_k, g^i{}_k$, and varied with respect to $\phi^i(r)$ under the constraints of incompressibility and the fact that the system is in contact with a bath of cations, anions, protons, and hydroxide ions. For the water density, the free energy minimization yields

$$\phi^i_w(r) = \rho^i_w(z)v_w = \exp\big(-\beta\pi^i(r)v_w\big), \quad (4)$$

whereas the density of the ions is given by

$$\rho^i_\alpha(r)v_w = \exp\big(\beta\big(\mu_\alpha - \mu^{\ominus}_\alpha\big) - \beta\pi^i(r)v_i - \beta\psi^i(r)z_\alpha e\big), \quad (5)$$

where z_α corresponds to the valence of the ion of type α. Functional variation of the free energy functional with respect to the electrostatic potential yields the Poisson equation containing the density of the ions from Eq. 5, together with the boundary conditions

$$-\varepsilon_0\varepsilon_m\frac{\partial\psi^m(r)}{\partial r}\bigg|_{r=R_{in}} + \varepsilon_0\varepsilon_w\frac{\partial\psi^{in}(r)}{\partial r}\bigg|_{r=R_{in}} = \sigma_{in}, \quad (6)$$

$$-\varepsilon_0\varepsilon_w\frac{\partial\psi^{out}(r)}{\partial r}\bigg|_{r=R_{out}} + \varepsilon_0\varepsilon_m\frac{\partial\psi^m(r)}{\partial r}\bigg|_{r=R_{out}} = \sigma_{out}, \quad (7)$$

$$\frac{\partial\psi^{in}(r)}{\partial r}\bigg|_{r=0^+} = 0 \quad \text{and} \quad \lim_{r\to\infty}\psi^{out}(r) = 0. \quad (8)$$

The solution of the electrostatic potential within the (capsid) spherical shell can be readily obtained, inasmuch as we assumed that there are no free charges within the shell ($\rho^m{}_q(r) = 0$) and is given by $\phi^m(r) = A/r + B$. The constants A and B can be obtained (self-consistently) via the boundary conditions.

Minimization with respect to the fraction of charged acid groups then yields

$$\frac{f^i_k}{1-f^i_k} = \frac{K_{a,k}}{[H^+]}e^{-\beta\pi_b v_{H^+}}e^{\beta e\psi(R_i)}, \quad (9)$$

where the experimental acid-base equilibrium constant is $K_{a,k} = C\exp(-\beta\Delta G^{\ominus}{}_{a,k})$, and $\Delta G^{\ominus}{}_{a,k}$ is the standard free energy change of the acid-base equilibrium reaction

$$R_kAH \rightleftarrows R_kA^- + H^+$$

of the carboxylic group of either aspartic or glutamic acid or the functional group of tyrosine (and cysteine) at infinite dilution, and C is a constant required for consistency of units and is equal to $C = 1/N_Av_w$, where N_A is Avogadro's number. The value π_b is the bulk osmotic pressure. A similar expression can be also obtained for the (de)protonation of the amine groups of the arginine, histidine, and lysine amino acids. (See Eq. S1 in the Supporting Material.)

Equation 9 should be compared to the degree of charge for an isolated acid molecule $f/(1-f) = K_a/[H^+]$. A similar equation without the osmotic pressure term was derived by Ninham and Parsegian (22) within their charge regulation theory to describe the acid-base equilibrium of lipid layers, and in Chan et al. (23,24), Boon and van Roij (25), and Netz (26). Equation 9 expresses the nonideal behavior of the dissociable groups of the amino acids found on the surface of the capsid (18,19,27). Note that the value of the surface potential $\psi(R_i)$ is not only influenced by the pH, but also by the salt concentration, the capsid size, and composition of capsid shell.

The unknowns in Eqs. 5–9 are the Lagrange multipliers or lateral pressures, $\pi(r)$ and the electrostatic potential, $\psi(r)$. Solutions of these variables can be obtained numerically (28). Details on the discretization procedure and numerical methods can be found in Nap et al. (18) and in the Supporting Material. The inputs required to solve the nonlinear equations are the bulk pH, the bulk salt concentration, the volume of the water molecule and the mobile ions, the surface densities of the amino-acid residues on the epitopal and hypotopal surface of the virus capsid, and the solution pK_a values of the dissociable groups (29). The surface densities of the capsid and the solution pK_a values are listed in Table S1 and Table S2.

RESULTS

Cysteine has a thiol with a functional end group that is a very weak acid, and this is usually not considered to be an acid at all. It is also reactive and can form disulfide bonds. It is appropriate, then, that we consider one case by taking into account the acidity of cysteine, and another in which we ignore the acidity of cysteine. We will therefore present two separate results for the amount of charge of the virus capsid.

Cysteine protonation

Fig. 2 shows the surface charge density for the inner and outer surfaces of the capsid as function of solution pH and salt concentration. For low pH, we observe that the inner as well as outer surface of the virus capsid are positive, whereas, for high pH, the capsid appears negatively charged. Interestingly, the surface charge density for a range of pH values shows an almost constant plateau. This effective charge plateau results also in a constant electrostatic surface potential as a function of pH that depends on the salt concentration. (See Fig. S1 in the Supporting Material.)

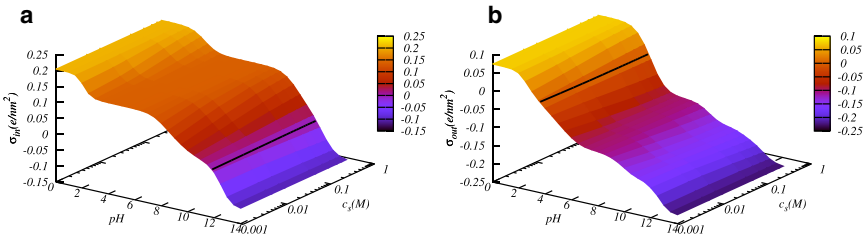

FIGURE 2 Surface charge density on (*a*) the inner (epitopal) and (*b*) outer (hypotopal) surfaces of the capsid as a function of solution pH and salt concentration. (*Solid lines*) Isoelectric points. The isoelectric point of the outer shell is located at pH $\simeq$ 3.8, whereas that of the inner shell is located at a distinctly different value of pH $\simeq$ 11.7. To see this figure in color, go online.

The plateau for the outer surface is more pronounced in the case where cysteine protonation is not considered (compare Fig. 2 with Fig. 6). This charge plateau obviously suggests a buffering behavior of the capsid charge under physiological pH and ionic strength conditions.

The effect of salt concentration on the surface charge density can be summarized as follows: with decreasing salt concentration, the absolute value of the surface charge is reduced. Following the behavior of the charge density, the surface electrostatic potential also increases with decreasing salt concentration. Only at very low pH and very high pH conditions does the surface charge remain approximately constant. Likewise, at the plateau, the value of the surface charge on the inner and outer surface of the virus capsid is relatively unaffected by changes in the salt concentrations.

To acquire more insight into the behavior of the surface charge density of the virus capsid, we present in Figs. 3–5 the contribution of individual amino acids to the total surface charge and the degree of deprotonation, with both as a function of pH at the physiological salt concentration of $c_s = 100$ mM. For pH values <2, only arginine and lysine contribute to the surface charge, inasmuch as only these amino acids are fully (positively) charged whereas all other amino acids are uncharged. For pH values between $2 \lessapprox$ pH $\lessapprox 5$, the aspartic acid and glutamic acid start to deprotonate and become negatively charged causing the total (outer) surface charge to drop.

We first describe the outer shell charge. At pH = 3.8, the epitopal charge density becomes zero, and for higher pH conditions, it becomes negative. For pH $\approx$ 5, almost all aspartic and glutamic amino acids are deprotonated and the epitopal surface charge density remains constant at a value $\sigma_{\text{in}} = -0.1$ e/nm^2 up to a pH value of pH $\approx$ 7–7.5. At pH $\approx$ 7.5, the cysteine amino acid starts to deprotonate, and the epitopal surface charge is lowered again. However, because the total amount of cysteine is less than the aspartic and glutamic acid combined (ratio $CYS{:}ASP + GLU \approx 1{:}3$), the lowering of the total surface charge is less dramatic than in the pH interval of $2 \lessapprox$ pH $\lessapprox 5$. Finally, at very high pH values of ~10 and 12, the arginine and lysine amino acids protonate and neutralize, resulting in a decrease of the number of positive charges. This leads to a further increase of the outer surface charge density to even larger negative values.

The inner surface charge density behaves globally similarly to the outer surface charge density; it changes from a positive value at low pH to a negative value at higher pH. However, the detailed behavior of the inner surface charge as a function of pH is in fact quite different from the outer surface charge, with the isoelectric point being reached at pH $\simeq$ 11.7, quite distinct from the pI value of the outer shell (see Fig. 3). The degree of charge of the inner surface can be found in Fig. S2. These differences arise because of the compositional difference between the epitopal and hypotopal surfaces. The inner surface has more arginines and lysines than the outer surface, whereas the inner surface has no glutamic and cysteine amino acids. On the contrary, the inner surface has tyrosines that are not present on the outer surface. Consequently, at low pH the inner surface charge density is larger than the outer surface charge density, and has a less negative value at higher pH values due to the absence of glutamic acid. Apart from the different values of pI, the most prominent difference between the hypotopal and epitopal effective charge is that the plateau of constant charge of the inner surface exists for a larger region of pH values than for the outer surface, primarily because of the absence of the negatively charged cysteine (Fig. 3).

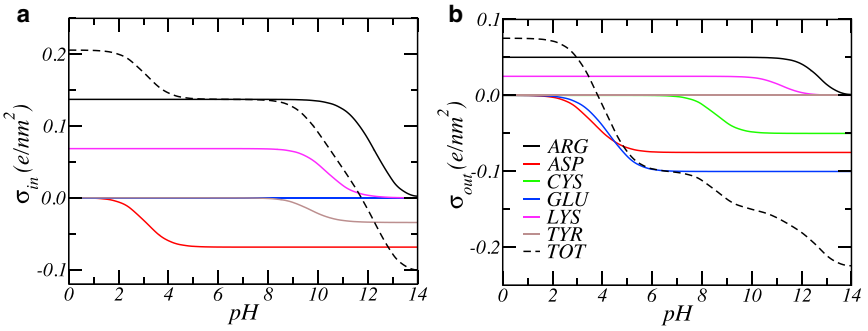

FIGURE 3 Contribution of different amino acids to the surface charge density on (*a*) the inner and (*b*) outer surfaces of the capsid as a function of solution pH. Cysteine acidity is considered. The salt concentration is $c_{\text{salt}} = 100$ mM. To see this figure in color, go online.

The general behavior of the surface charge and electrostatic surface potential as a function of salt concentration and pH can be understood as follows: The amount of charge, or more specifically the degree of (de)protonation of the amino acids, occurs through a balance with the chemical free energy of the acid-base equilibrium reaction of the involved amino acids, the electrostatic interactions, and the mixing entropy of the mobile ions (or, more precisely, the entropy associated with counterion confinement). With decreasing salt concentrations, the electrostatic interaction between the charged surface groups are less screened and the system needs to compensate for the increased electrostatic repulsions.

The virus capsid system can respond in two possible ways:

1. Recruit additional counterions from the bulk reservoir to increase the electrostatic screening. This decrease in enthalpic repulsion occurs at an entropic penalty due to the loss of translational entropy of the counterions.
2. Mitigate the electrostatic repulsions by reducing the total surface charge of the virus capsid, which can be accomplished by regulating or shifting the acid-base equilibria of the various amino acids at the cost of chemical free energies.

The mechanism of charge regulation is usually the primary mode by which charged systems in general and the virus capsid as well try to reduce the effects of electrostatic repulsions, arising from the lower cost associated with the chemical contribution as compared to the counterion confinement. The charge regulation also results in a strongly position-dependent pH and electrostatic potential. A typical example is presented in Fig. S3.

The charge regulation mechanism of the amino acids on the outer surface is illustrated in Figs. 4 and 5. It shows the degree of deprotonation of the different amino acids as functions of pH. The solid lines correspond to the solution of Eq. 9 and Eq. S1 in the Supporting Material and the dotted lines correspond to the case where the degree of deprotonation of the amino acids obeys the (bulk) Henderson-Hasselbalch equation valid in an infinite dilute solution. Because the amino acids are not in dilute solution but located on the inner and outer surface of the virus capsid while strongly interacting with each other, the amount of charge of the amino acids significantly deviates from their ideal solution behavior. At low pH, the (aspartic) amino acids shift its degree of deprotonation up, resulting in higher amounts of negative charge that compensate the positive charges of the (protonated) amine groups of arginine and lysine (see Fig. 4). Glutamic acid behaves similar to aspartic acid, as shown in Fig. 3 and Fig. S4, because it carries a similar carboxylic acid.

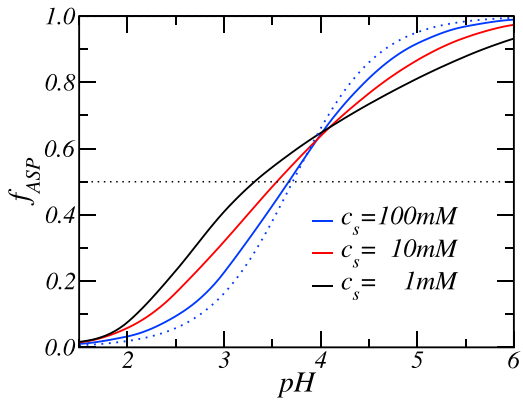

FIGURE 4 The degree of deprotonation of aspartic acid on the outer surface of the capsid as a function of solution pH for various salt concentrations. Cysteine acidity is considered. (*Dotted line*) Degree of charge that aspartic acid would have in a dilute solution. To see this figure in color, go online.

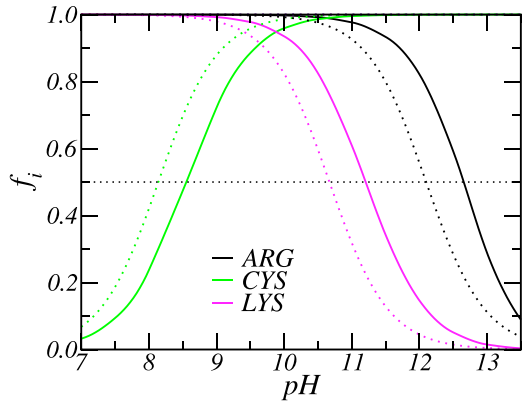

FIGURE 5 The degree of deprotonation of the different amino acids on the outer surfaces of the capsid as a function of solution pH. Cysteine acidity is considered. The salt concentration is c_s = 100 mM. (*Dotted lines*) Degree of charge that the amino acid would have in a dilute solution. To see this figure in color, go online.

The charge regulation of the inner aspartic acid and outer aspartic and glutamic amino acid are different in extent and direction for pH $\gtrapprox$ 3.5. For a large pH interval, the aspartic acid located on the inner surface has a larger degree of charge than expected, based on the ideal solution Henderson-Hasselbalch behavior (see Fig. S2). Moreover, the aspartic and glutamic acid found on the outer surface for pH $\gtrapprox$ 4 reverse their behavior, and their amount of charging is less than expected from the ideal behavior. This is due to the fact that the overall outer surface charge has become negative for bulk pH conditions above pH $\gtrapprox$ 4 (see Fig. 4), hence the system tries to reduce the total amount of negative charge by shifting the acid-base equilibrium toward the uncharged state of the aspartic and glutamic acid.

For the inner surface, this reversal from upregulation to downregulation does not occur because the total amount of aspartic acid present on the inner surface is less than the total amount of (positively charged) arginine and lysine. For pH $>$ 6, essentially all aspartic amino acids are charged,

whereas the total amount of charge on the inner surface is still positive. Starting from pH $\approx$ 7, the tyrosine amino acids acquire charges to reduce the overall amount of positive charge. Tyrosine behaves similarly to aspartic acid located on the inner surface of the capsid. However, concomitant with the increase in the degree of charge of the tyrosine amino acid, the lysine amino acid will shift its acid-base equilibrium toward the neutral state. The increase in negative charges of tyrosine, and decrease of the amount of positively charged lysine and, to a lesser extent, the decrease in the amount of positively charged arginine amino acids, results in a reduction of the amount positive charge on the inner surface. At approximately pH = 12, the system is neutralized, and for larger pH values, the inner surface becomes negatively charged. The acid-base equilibrium of lysine and arginine shift to a state of higher amount of protonated positive charge to compensate for the excess total negative charge on the outer surface.

The general charging behavior of the epitopal surface of the capsid at higher pH follows a similar charging mechanism as outlined before for the hypotopal surface. However, there are also noticeable differences. Most importantly, the outer surface has many more aspartic and glutamic amino acids, hence at approximately pH = 6–7 the outer surface is already negatively charged. Therefore, at pH values pH $\gtrapprox$ 10 and higher, lysine and arginine shift to a higher degree of protonated positive charge to compensate for the excess total negative charge on the outer surface. The shifts are larger than observed on the inner surface. For example for pH = 11, the degree of charge of lysine is $f_{\mathrm{LYS}} = 0.6$ compared to ideal solution charge of $f_{\mathrm{LYS}} = 0.32$. At pH = 11, the inner surface lysine amino acids are still downregulating, inasmuch as the total charge is still positive, but the changing is more modest: $f_{\mathrm{LYS}} = 0.23$.

Another important difference is the presence of cysteine on the outer surface of the capsid. Taking into account the potential protonation of cysteine leads to additional negative charges on the outer surface. In the pH interval from 7 to roughly 11, cysteine amino acids try to compensate for the electrostatic repulsions by shifting their degree of charging toward the neutral state. For higher pH values, the chemical energy is so large that only a small shift suffices to compensate for the additional electrostatic interactions, and essentially, all cysteine amino acids are charged. This applies just as well to aspartic and glutamic acids.

The changes in degree of protonation of the amino acids not only depend critically on the pH but also on the ionic strength of the solution. This dependence is demonstrated in Fig. 4 showing the degree of dissociation of aspartic acid. With decreasing salt concentration, the change or shift of the acid-base equilibrium away from its ideal solution behavior grows larger. Other amino acids have similar large shifts in the degree of protonation. (See Fig. S5 showing the degree of protonation as function of salt concentration for lysine.) The degree of protonation of the amino acids shifts by 1–1.5 pH units. Its shape not only changes quantitatively but also qualitatively. For decreasing salt concentrations, the shape of the degree of protonation curve of the aspartic amino acid strongly deviates from, and is much broader than, the curve for ideal solution behavior. This implies that although the ideal behavior informs us that a single acid is charged or uncharged, the same information is not contained within the degree of charge of amino acids on the capsid inasmuch as the pH interval required to change the amino acids from uncharged to charged is much larger. This demonstrates the importance of both charge regulation and counterion release in properly predicting the degree of charge of the capsid.

In summary, the proteinaceous capsid regulates the amount of charge of the various amino acids in such a way as to avoid large electrostatic repulsions. The degree of charge on the amino acids is therefore shifted to reduce the total amount of surface charge. Moreover, it shows buffering behavior under physiological conditions of pH and ionic strength. Note that although a completely neutralized system would minimize the electrostatic repulsions, this can only occur at a very large chemical free energy penalty of the protein acid-base equilibria. Instead, the system minimizes the global free energy by finding the least-frustrated state by compromising and balancing among the chemical free energy, the electrostatic energy, and the translational entropy of the mobile ions.

No cysteine protonation

During investigation of the effect of coat protein disulfide cross-links on the stability of PP7 phages, Caldeira and Peabody (30) found that thermally stable PP7 phages would lose their stability if exposed to a detergent that could destroys disulfide bonds. These experiments indicate that the functional thiol end group of cysteine is reactive and can form disulfide bonds. Hence, one can consider whether the functional group of cysteine also contributes to the surface charge. We therefore consider the case of variable acidity of the cysteine amino acid. For low pH values, we find identical behavior in the cases with or without the (de)protonation of cysteine (see Fig. 6 (and Fig. S6)). For pH values <7, cysteine is neutral and in its protonated state; hence, the surface charge and potential are not affected. For higher pH conditions, we observe differences if we do not allow for the variable acidity of the cysteine.

In the absence of the deprotonatable cysteine groups, we observe a smaller negative outer surface charge. Moreover, it is constant for a much larger region of pH, indicating that buffering is also operating within physiological conditions. The effect on the inner surface charge is minimal because

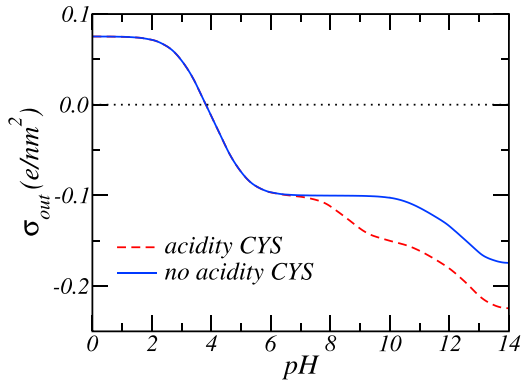

FIGURE 6 Surface charge density on the outer part of the capsid as a function of solution pH for a salt concentration of $c_s = 100$ mM, taking into account the possibility of cysteine protonation (*red curve*) and the case in which we ignore the acidity of cysteine (*blue curve*). To see this figure in color, go online.

there is no cysteine amino acid on the inner surface part of the capsid.

OTHER BACTERIOPHAGES

Different bacteriophages have different distributions of amino acids. This difference in the composition of the capsid results in significant changes in both the size and the sign of outer and inner surface charge density, as illustrated in Fig. 7. It shows the surface charge density of the inner surface density for a number of different bacteriophages. The outer surface charge density of the bacteriophages is presented in Fig. S7 along with their amino-acid compositions. (See Table S3, Table S4, Table S5, Table S6, Table S7, and Table S8.)

Although the bacteriophages labeled FA, GA, MS2, and PPR1 have different AA compositions compared to PP7, they are similar in size and symmetry. On the other hand, the p22 procapsid and epsilon 15 capsid are greater than two-times larger and have a $T = 7$ instead of a $T = 3$ symmetry. All phages were selected to be approximately spherical as expressed by their relative low Föppl-von Kármán numbers (31). (See Table S9.) Acidity of cysteine is not taken into account, because only pp7, ε15, and p22 procapsid contain cysteine. However, its effect is small for the latter two, inasmuch as they contain only small amounts of cysteine. We observed that the functional variation of charge with pH and ionic strength is similar for all phages: their capsids are positively charged at low pH and negatively charged capsid at high pH, reflecting the charge states of amines and carboxylic acid at low and high pH values. However, the exact amount of surface charge is specific for a given bacteriophage so that different capsids have very different amounts of charge and can even have different signs of charge at a set value of pH.

The ε15 and p22 capsids at physiological pH are negatively charged on the inside, whereas the other phages are positively charged. The latter capsids self-assemble spontaneously with its ssRNA genomic material, whereas ε15 and p22 capsids use molecular motors to load their dsDNA cargo. The negative sign of the inner surface charge is correlated with the work required to load these capsids with their genomic material. A preliminary calculation—beyond the scope of this work—shows that adding a uniform negative charge inside the (P22) capsid, corresponding to the dsDNA cargo, to the inside of the (p22) capsid, results in a decrease and even reversal of the inner

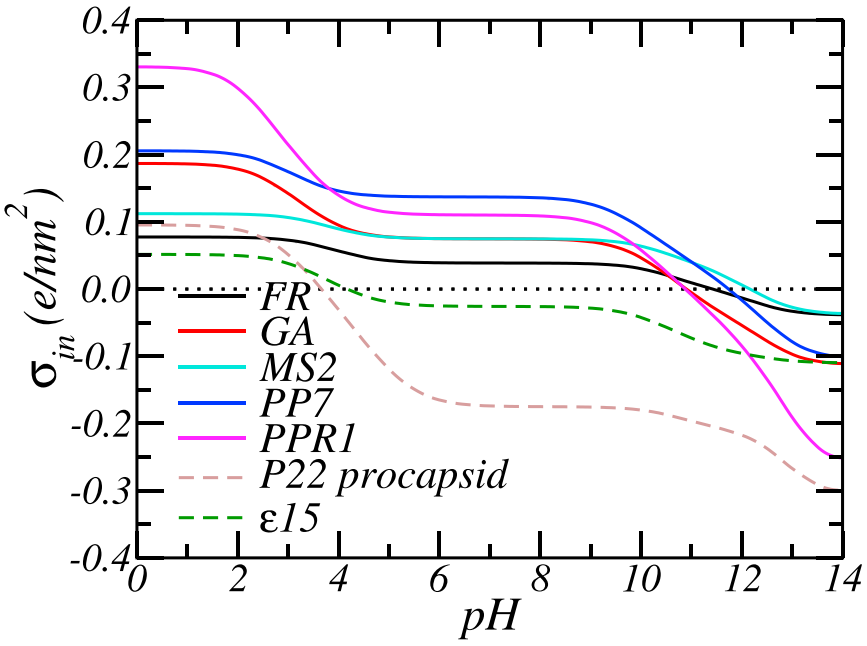

FIGURE 7 Surface charge density on the inner part of the various bacteriophage capsids as a function of solution pH for a salt concentration of $c_s = 100$ mM. To see this figure in color, go online.

charge, due to the charge-regulating ability of the AAs. (See Fig. S8.)

DISCUSSION

In a simplified treatment, taking into account only the charge on five amino acids at physiological pH, the PP7 bacteriophage was found to carry surface charge densities of $\sigma_{in} = -0.14\ e/\text{nm}^2$ and $\sigma_{out} = 0.1\ e/\text{nm}^2$ (6). Our calculations support these previous findings inasmuch as they predict the same surface charge density at physiological conditions for outer as well as inner surface of the capsid. This agreement is gratifying, but maybe not surprising, in light of the fact that at physiological conditions all amino acids on the outer surface are completely charged except for cysteine, which is almost uncharged. When the acidity of cysteine is considered explicitly, the changes are quite distinct (Fig. 6). In general, the surface charge density seems to level off at a range of pH values, which is different for the hypotopal and epitopal surface layers, with the effect of pH as well as of the ionic strength being very large, introducing qualitative changes in the charging state of the capsid proteins.

The phage PP7 is usually assembled in vitro at a slightly basic pH of 8.0–8.5 (30,32). Michen and Graule (7) report the isoelectric point of the phage to be in the range of 4.3–4.9. These measured values were obtained for different concentrations of NaCl (0, 40, 100 mM), with the buffer composition fixed. It appears that the isoelectric point actually moves toward lower values as the salt concentration increases (33).

Here, we find the isoelectric point of the virus capsid is located at approximately $\text{pI} = 3.85$ for a salt concentration of $c_s = 100$ mM. It increases to $\text{pI} = 3.95$ for a salt concentration of $c_s = 1$ mM (see Fig. S9). Following the experimental observations (33), the predicted isoelectric point of the capsid also decreases with increasing salt concentration. The value of the isoelectric point is slightly less than the observed pI. We speculate that this difference occurs because we assumed that there were no free charges within the shell. In reality, there are charges within the shell that will influence the amount of the surface charge, and, hence, alter the isoelectric point. Also, equally important, the assumption of a homogenous surface charge distribution and the fact that all amino-acid charges are located on a spherical shell instead of being radially distributed influences the electrostatic interactions and affect the degree of charge and the location of the isoelectric point.

We also detect a vastly different value for the hypotopal shell isoelectric point, $\text{pI}_{in} \simeq 11.75$, as compared to the epitopal shell. Although the different amino-acid compositions of both shells certainly explain the difference, it would be interesting to speculate whether the isoelectric point of the inner shell is in fact closely related to the fact the it comes into close contact and interacts strongly with the negatively charged nucleic-acid cargo of the bacteriophage. The electrostatic stabilization of the virion itself might thus stipulate that the inner isoelectric point differs substantially from the outer one. As far as we know, this is the first instance where a substantial difference between the epi- and hypotopal isoelectric points have been calculated, inasmuch as experimentally they would be quite difficult to measure. It would be interesting to explore further this point by introducing a negatively charged flexible polymer into the interior of the capsid and analyze its free energy.

Understanding the behavior of the isoelectric point of viruses also seems to be interesting from several other perspectives as well, whether it be the electrical detection of single viruses (34), adsorption and transport of viruses in different materials (35), or the impact of charge and the isoelectric point of epitopes on virus-host interactions (36). For all these situations, knowing how the surface charge varies with pH and what the effective pI of the epitope would be can prove very relevant.

CONCLUDING REMARKS

We have investigated and quantified the effect of pH and ionic strength on the charge distributions of the bacteriophage PP7 capsid. We used a molecular theory, previously devised to study various interfacial polymer problems such as the ion-conductivity of polyelectrolyte of modified nanopores, the adsorption of proteins to polymer layers, and charge regulation of acid-coated nanoparticles (27,37,38). In this context we explicitly account for the charge distribution of the amino acids of this specific bacteriophage capsid. We therefore do not make any assumptions regarding the charging state of the various amino acids, but instead predict the charging state of the epi- and hypotope based on their distribution over the outer and inner surfaces of the capsid. In such respect, this article can be seen as an extension of the seminal studies performed by Katchalsky et al. (39,40) on the behavior of weakly charged biopolymers as well as of the work by Ninham and Parsegian (22) describing the acid-base equilibrium of surfaces bearing dissociable groups.

Our main finding is that solution pH as well as salt ionic strength both exhibit a very large effect and introduce qualitative changes in the charge state of the capsid, which can switch from net positive to net negative, depending on the characteristics of the solution. The charge state of the virus capsid is shown to arise from a rather delicate balance between the chemical dissociation equilibrium of the amino acids and the electrostatic interaction between surface charges mediated by mobile salt ions and their translational entropy. The article conclusively demonstrates that to understand the nature and magnitude of the capsid charge, one needs to consider molecular details such as the acid-base equilibrium of the amino acids and their exact distribution across the capsid wall to properly understand the charge

state of the virus capsid. These conclusions are also completely vindicated by recent experiments on electrophoretic mobilities of cowpea chlorotic mottle viruses viral capsids and their capsid proteins (11), which make it clear that the sign and the magnitude of the capsid charge depends on the solution pH and ionic strength in exactly the same way as described with our theory.

An important backdrop to which this study and its possible generalizations are bound to contribute some much-needed conceptual and formal framework, is the gene delivery context. This revolves around the conditions for assembly of a viruslike nanoparticle that would yield a stable product in blood circulation while being prone to spontaneously disassemble at the target site, specifically in the tumor microenvironment or the endolysosomal compartment of the tumor cell (14). The connecting line with our analysis presented above is the fact that the blood pH is regulated tightly within the interval 7.35–7.45 at an ionic strength of 0.1–0.2 M, whereas the typical solution conditions of the endolysosome of the tumor cell are pH 5.0 and an ionic strength of 0.05–0.1 M. The knowledge and prediction of the stability of the viruslike nano particles hinges upon the evaluation of the effects of the pH and ionic strength of the solution on the sign and magnitude of the capsid charges. Our results are the first step toward this goal in the sense that we have formulated a theory that gives us the effective capsid charge densities as functions of solution conditions. What remains to be investigated is the next step, which goes from the specification of charges to the evaluation of the stability phase diagram of either the empty capsid or an entire virion with its genome cargo.

Although we have added important molecular details to the fundamental theoretical description of the virus capsid, it should be realized that it is nevertheless still only approximate. Furthermore, to make it tractable, we made a number of simplifying assumptions: the shell of capsid is considered to be rigid and spherical; the interior of the capsid is empty; and the charge distribution is homogeneous along, but not across, the capsid wall. In potential future directions of research, we can address the generalizations of a number of these assumptions. For example, one can consider the effect of loading the capsid with RNA (polymer) cargo. The presence of this molecular cargo will change the dielectric and osmotic environment of the interior of the capsid, which will furthermore affect electrostatic interactions and shift the acid-base equilibrium of the amino acids. Inasmuch as the molecular theory was developed for polymers (18), such extension of the theory is indeed quite straightforward. Similarly, in future work it will be important to specifically consider the positions of the amino acids to explore what the effects of an inhomogeneous amino-acid distribution are on the degree of charge of the capsid. Our work can be thus seen as the first step toward a deeper understanding of the behavior of virus capsids, based on a more detailed molecular description of its constituent molecules than is usually assumed.

SUPPORTING MATERIAL

Nine tables, nine figures, and four equations are available at http://www.biophysj.org/biophysj/supplemental/S0006-3495(14)00937-0.

We are grateful to A. Šiber for making the images of the PP7 bacteriophage density and charge distribution. R.P. also thanks Prof. Nicole F. Steinmetz for many discussions regarding fundamental problems in viral nanoparticle assembly.

A.L.B. acknowledges support by Slovene Agency for Research and Development through grants No. P1-0055 and J1-4297. R.P. acknowledges support in the study of long-range interactions for biomolecular and inorganic nanoscale assembly by the U.S. Department of Energy, Office of Basic Energy Sciences, Division of Materials Sciences and Engineering under award No. DE-SC0008176. I.S. acknowledges support from National Science Foundation grant No. CBET-1403058.

REFERENCES

1. Walker, D. A., B. Kowalczyk, …, B. A. Grzybowski. 2011. Electrostatics at the nanoscale. *Nanoscale.* 3:1316–1344.
2. French, R. H., V. A. Parsegian, …, T. Zemb. 2010. Long range interactions in nanoscale science. *Rev. Mod. Phys.* 82:1887–1944.
3. Šiber, A., A. L. Božič, and R. Podgornik. 2012. Energies and pressures in viruses: contribution of nonspecific electrostatic interactions. *Phys. Chem. Chem. Phys.* 14:3746–3765.
4. Prinsen, P., P. van der Schoot, …, C. M. Knobler. 2010. Multishell structures of virus coat proteins. *J. Phys. Chem. B.* 114:5522–5533.
5. Kegel, W. K., and P. van der Schoot. 2006. Physical regulation of the self-assembly of tobacco mosaic virus coat protein. *Biophys. J.* 91:1501–1512.
6. Lošdorfer Božič, A., A. Šiber, and R. Podgornik. 2012. How simple can a model of an empty viral capsid be? Charge distributions in viral capsids. *J. Biol. Phys.* 38:657–671.
7. Michen, B., and T. Graule. 2010. Isoelectric points of viruses. *J. Appl. Microbiol.* 109:388–397.
8. Lavelle, L., M. Gingery, …, J. Ruiz-Garcia. 2009. Phase diagram of self-assembled viral capsid protein polymorphs. *J. Phys. Chem. B.* 113:3813–3819.
9. Adolph, K. W., and P. J. G. Butler. 1974. Studies on the assembly of a spherical plant virus. I. States of aggregation of the isolated protein. *J. Mol. Biol.* 88:327–341.
10. Jończyk, E., M. Kłak, …, A. Górski. 2011. The influence of external factors on bacteriophages—review. *Folia Microbiol. (Praha).* 56: 191–200.
11. Vega-Acosta, J. R., R. D. Cadena-Nava, …, J. Ruiz-García. 2014. Electrophoretic mobilities of a viral capsid, its capsid protein, and their relation to viral assembly. *J. Phys. Chem. B.* 118:1984–1989.
12. Cuellar, J. L., F. Meinhoevel, …, E. Donath. 2010. Size and mechanical stability of norovirus capsids depend on pH: a nanoindentation study. *J. Gen. Virol.* 91:2449–2456.
13. Cuillel, M., C. Berther-Colominas, …, M. Zulauf. 1987. Reassembly of brome mosaic virus from dissociated virus. *Eur. Biophys. J.* 15:169–176.
14. N. F. Steinmetz, and M. Manchester, editors 2011. Viral Nanoparticles: Tools for Materials Science and Biomedicine. Pan Stanford Publishing, Singapore.
15. Daniel, M.-C., I. B. Tsvetkova, …, B. Dragnea. 2010. Role of surface charge density in nanoparticle-templated assembly of bromovirus protein cages. *ACS Nano.* 4:3853–3860.

16. Lin, H.-K., P. van der Schoot, and R. Zandi. 2012. Impact of charge variation on the encapsulation of nanoparticles by virus coat proteins. *Phys. Biol.* 9:066004.

17. Belyi, V. A., and M. Muthukumar. 2006. Electrostatic origin of the genome packing in viruses. *Proc. Natl. Acad. Sci. USA.* 103:17174–17178.

18. Nap, R., P. Gong, and I. Szleifer. 2006. Weak polyelectrolytes tethered to surfaces: effect of geometry, acid-base equilibrium and electrical permittivity. *J. Polym. Sci. B Polym. Phys.* 44:2638–2662.

19. Nap, R. J., and I. Szleifer. 2013. How to optimize binding of coated nanoparticles: coupling of physical interactions, molecular organization and chemical state. *Biomater Sci.* 1:814–823.

20. Schwinger, J., L. L. DeRaad, Jr., …, W.-Y. Tsai. 1998. Classical Electrodynamics. Perseus Books, Reading, Massachusetts.

21. Javidpour, L., A. Lošdorfer Bozic, …, R. Podgornik. 2013. Multivalent ion effects on electrostatic stability of virus-like nano-shells. *J. Chem. Phys.* 139:154709.

22. Ninham, B. W., and V. A. Parsegian. 1971. Electrostatic potential between surfaces bearing ionizable groups in ionic equilibrium with physiologic saline solution. *J. Theor. Biol.* 31:405–428.

23. Chan, D., J. W. Perram, …, T. W. Healy. 1975. Regulation of surface potential at amphoteric surfaces during particle-particle interaction. *J. Chem. Soc, Faraday Trans. I.* 71:1046–1057.

24. Chan, D., T. W. Healy, and L. R. White. 1976. Electrical double layer interactions under regulation by surface ionization equilibria-dissimilar amphoteric surfaces. *J. Chem. Soc. Faraday Trans. I.* 72:2844–2865.

25. Boon, N., and R. van Roij. 2011. Charge regulation and ionic screening of patchy surfaces. *J. Chem. Phys.* 134:054706.

26. Netz, R. R. 2003. Charge regulation of weak polyelectrolytes at low- and high-dielectric-constant substrates. *J. Phys. Condens. Matter.* 15:S239–S244.

27. Wang, D., R. J. Nap, …, I. Szleifer. 2011. Why and how nanoparticle's curvature regulates the apparent pK_a. *J. Am. Chem. Soc.* 133:2192–2197.

28. Hindmarsh, A. C., P. N. Brown, …, C. S. Woodward. 2005. SUNDIALS: suite of nonlinear and differential/algebraic equation solvers. *ACM Trans. Math. Softw.* 31:363–396.

29. D. R. Lide, editor 2013. CRC Handbook of Chemistry and Physics, 94th Ed. CRC Press, Boston, MA.

30. Caldeira, J. C., and D. S. Peabody. 2007. Stability and assembly in vitro of bacteriophage PP7 virus-like particles. *J. Nanobiotechnol.* 5:10.

31. Lošdorfer Božič, A., A. Šiber, and R. Podgornik. 2013. Statistical analysis of sizes and shapes of virus capsids and their resulting elastic properties. *J. Biol. Phys.* 39:215–228.

32. Tars, K., K. Fridborg, …, L. Liljas. 2000. Structure determination of bacteriophage PP7 from *Pseudomonas aeruginosa*: from poor data to a good map. *Acta Crystallogr. D Biol. Crystallogr.* 56:398–405.

33. Brorson, K., H. Shen, …, D. D. Frey. 2008. Characterization and purification of bacteriophages using chromatofocusing. *J. Chromatogr. A.* 1207:110–121.

34. Patolsky, F., G. Zheng, …, C. M. Lieber. 2004. Electrical detection of single viruses. *Proc. Natl. Acad. Sci. USA.* 101:14017–14022.

35. Dowd, S. E., S. D. Pillai, …, M. Y. Corapcioglu. 1998. Delineating the specific influence of virus isoelectric point and size on virus adsorption and transport through sandy soils. *Appl. Environ. Microbiol.* 64:405–410.

36. Bendahmane, M., M. Koo, …, R. N. Beachy. 1999. Display of epitopes on the surface of tobacco mosaic virus: impact of charge and isoelectric point of the epitope on virus-host interactions. *J. Mol. Biol.* 290:9–20.

37. Satulovsky, J., M. A. Carignano, and I. Szleifer. 2000. Kinetic and thermodynamic control of protein adsorption. *Proc. Natl. Acad. Sci. USA.* 97:9037–9041.

38. Tagliazucchi, M., O. Peleg, …, I. Szleifer. 2013. Effect of charge, hydrophobicity, and sequence of nucleoporins on the translocation of model particles through the nuclear pore complex. *Proc. Natl. Acad. Sci. USA.* 110:3363–3368.

39. Katchalsky, A., N. Shavit, and H. Eisenberg. 1954. Dissociation of weak polymeric acids and bases. *J. Polym. Sci., Polym. Phys.* 13:69–84.

40. Katchalsky, A. 1971. Polyelectrolytes. *Pure Appl. Chem.* 26:327–373. http://dx.doi.org/10.1351/pac197126030327.